

Supplementary Information for

**Self-Driven SnS_{1-x}Se_x Alloy/GaAs Heterostructure based Unique
Polarized Sensitive Photodetectors**

Mengmeng Yang¹, Wei Gao^{2,3*}, Mengjie He⁴, Shuai Zhang², Ying Huang², Zhaoqiang Zheng^{1*}, Dongxiang Luo^{2,3}, Fugen Wu¹, Congxin Xia⁴, Jingbo Li^{2,3*}

¹ Guangdong Provincial Key Laboratory of Information Photonics Technology, School of Materials and Energy, Guangdong University of Technology, Guangzhou, 510006, Guangdong, P. R. China.

² Institute of Semiconductors, South China Normal University, Guangzhou, 510631, Guangdong, P. R. China.

³ Guangdong Key Lab of Chip and Integration Technology, Guangzhou 510631, P.R. China.

⁴ Physics and Electronic Engineering College, Henan Normal University, Xinxiang 453007, P. R. China.

***Corresponding authors:**

Zhaoqiang Zheng, Email: zhengzhq5@mail2.sysu.edu.cn;

Wei Gao, Email: gaowei317040@m.scnu.edu.cn;

Jingbo Li, Email: jbli@m.scnu.edu.cn

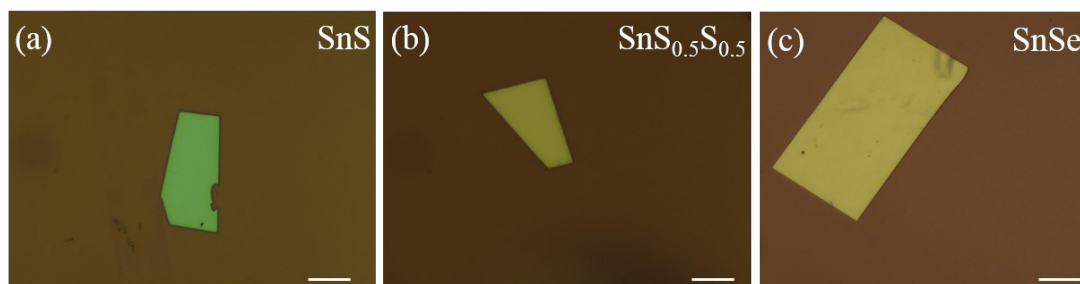


Figure S1. Optical images of (a) SnS, (b) SnS_{0.5}Se_{0.5}, (c) SnSe nanosheets

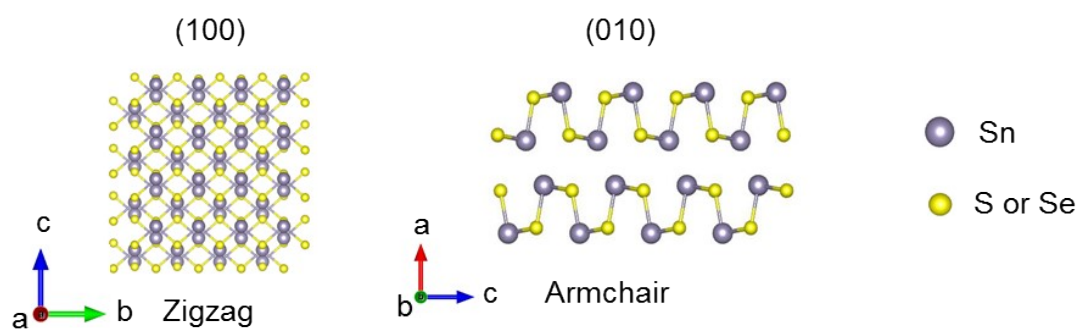


Figure S2. Atomic model of a bulk SnS_{0.5}Se_{0.5} crystal structure viewed along the (100) or (010) directions.

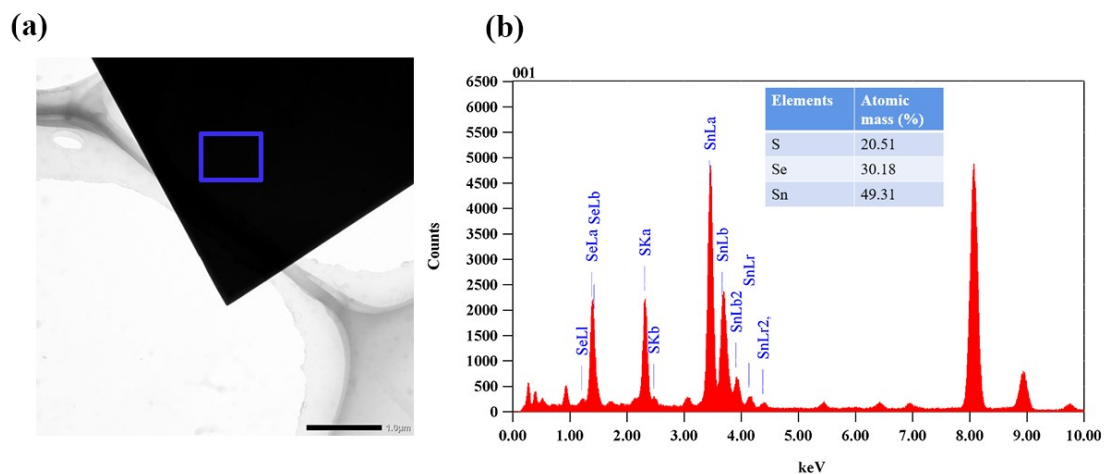


Figure S3. (a) HRTEM image and (b) The corresponding EDS spectrum and the extracted EDS data of SnS_{0.5}Se_{0.5} nanosheets in the blue square.

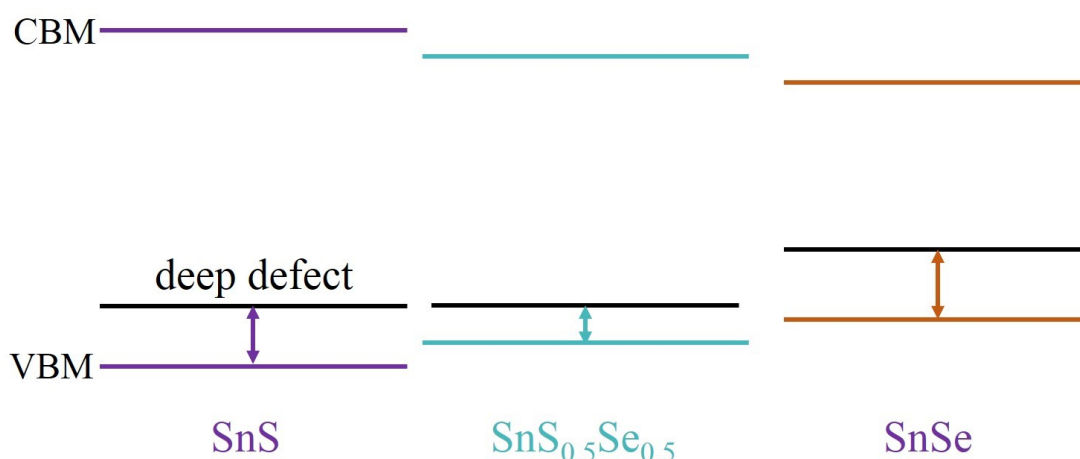


Figure S4. Schematic plot of the energy band and deep defect level for SnS, SnS_{0.5}Se_{0.5} and SnSe.

The deep-level defects of binary SnS and SnSe become harmful recombination centers, which greatly reduce the possibility that the captured holes will be emitted into the conduction band and become free holes again¹. After alloying, the energy state of CBM and VBM of SnS_{0.5}Se_{0.5} lies between the binary SnS and SnSe, so the deep-level defects getting low, results in the captured holes in the defect states tend to flow to the VBM to become free holes.

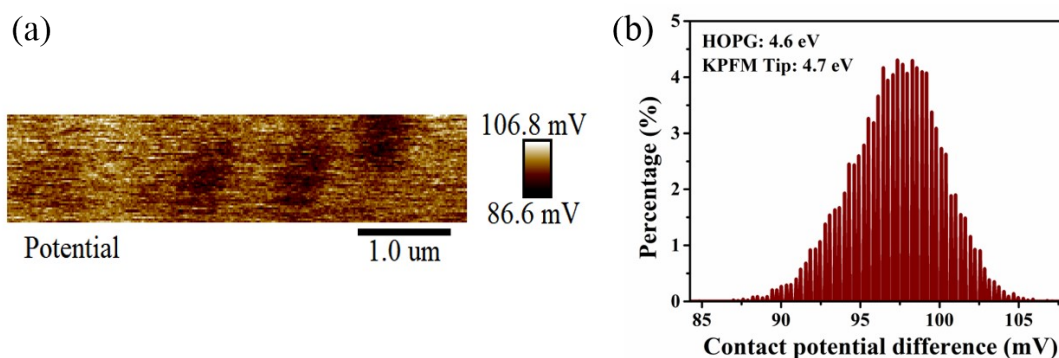


Figure S5. (a) The corresponding spatial distribution of surface potential of HOPG by KPFM. (B) Histogram of contact potential difference of the HOPG surface.

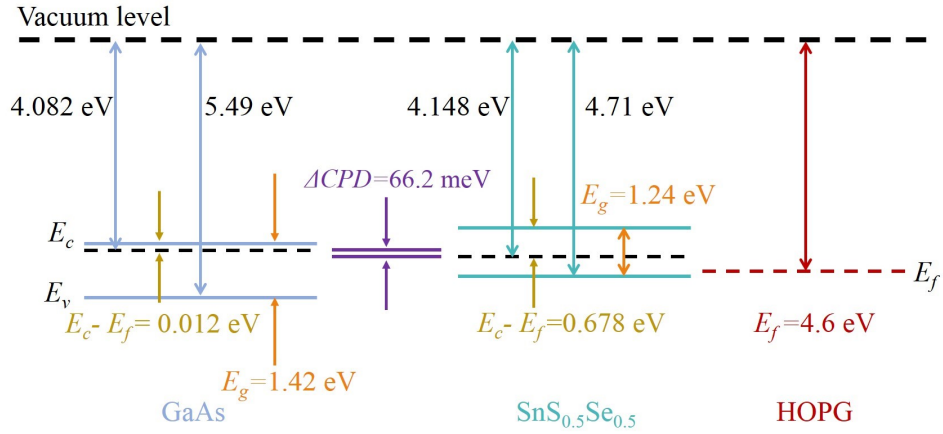


Figure S6. Energy band alignments of SnS_{0.5}Se_{0.5}/GaAs device by KPFM.

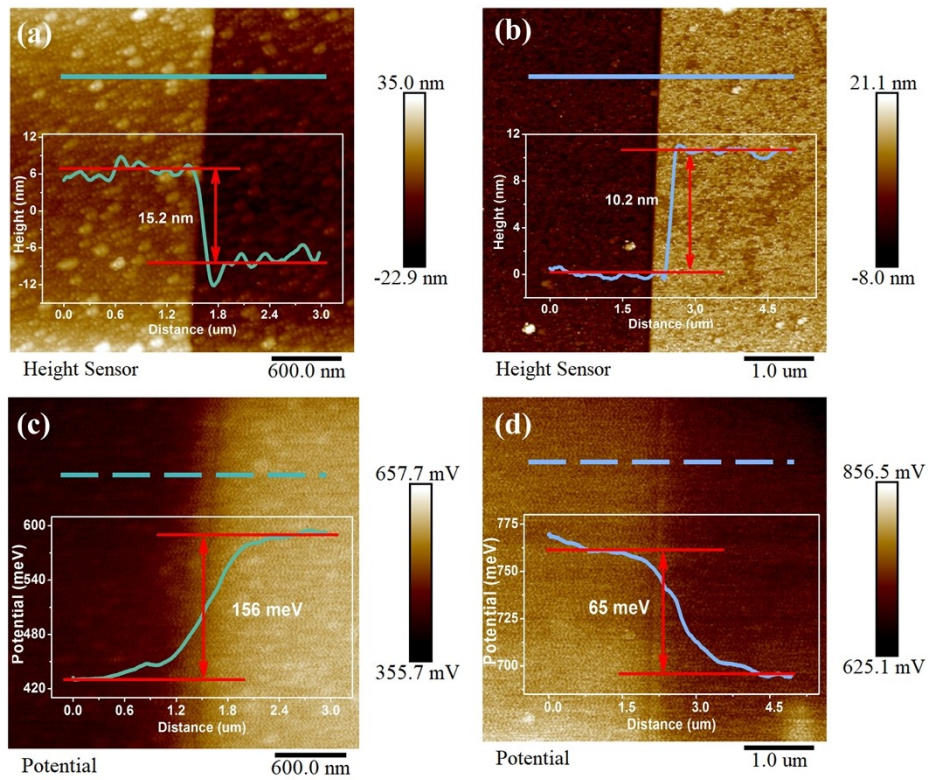


Figure S7. (a) and (b) AFM image with the thickness profile obtained from the AFM image along the straight line of the SnS/GaAs, and SnSe/GaAs heterostructures, respectively. (c) and (d) The corresponding spatial distribution of surface potential of the SnS/GaAs, and SnSe/GaAs heterostructures along the dashed line.

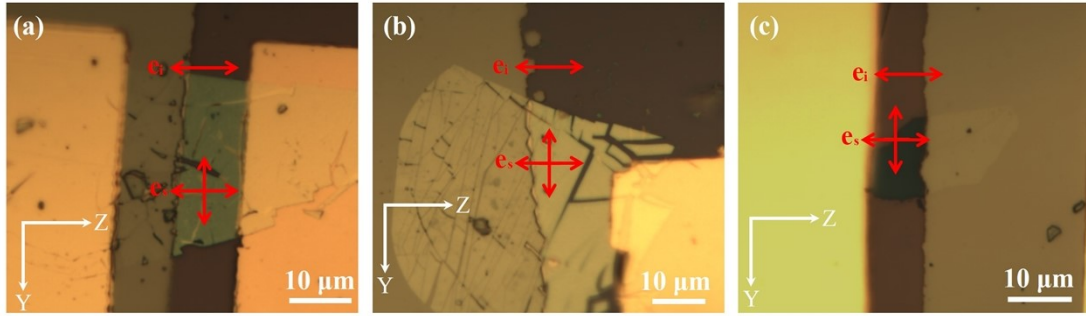


Figure S8. (a)-(c) Optical image of the measured SnS, SnS_{0.5}Se_{0.5} and SnSe nanosheets, showing the crystallographic axes, the polarized direction of the incident laser and scattered light.

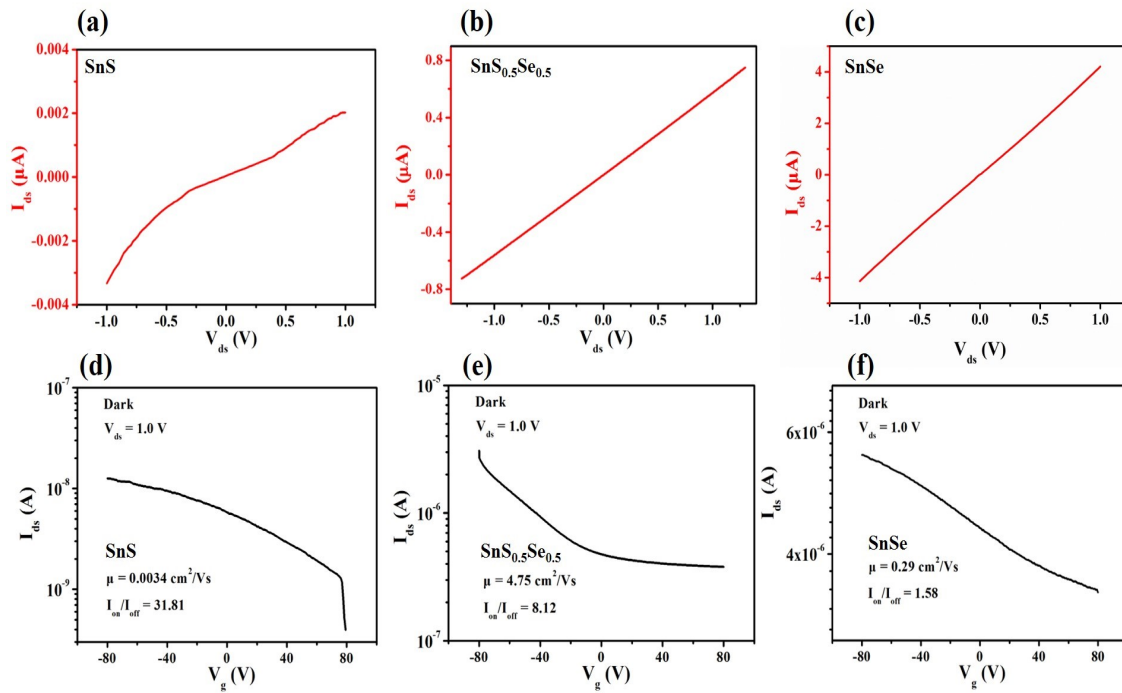


Figure S9. (a)-(c) I_{ds} - V_{ds} curves and (d)-(f) transfer characteristic curves of pure SnS, SnS_{0.5}Se_{0.5}, SnSe under dark. Mobility of the SnS_{0.5}Se_{0.5} has increased obviously.

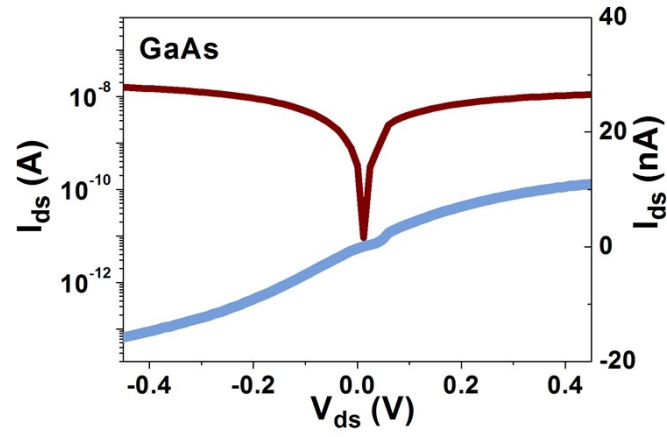


Figure S10. I_{ds} - V_{ds} curves of Au/GaAs at linear and logarithmic forms.

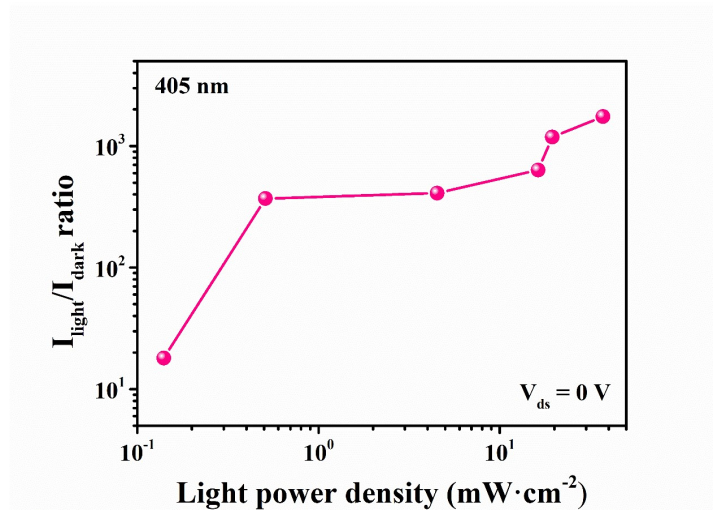


Figure S11. Incident light intensity dependence of I_{light}/I_{dark} ratio at the bias of 0 V.

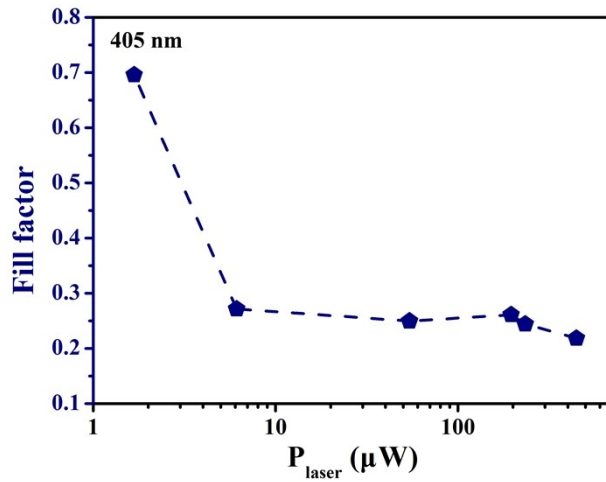


Figure S12. Power dependent fill factor (FF) of the heterostructure device. The FF can be calculated as²:

$$\text{FF} = P_{\text{max}} / (I_{\text{sc}} V_{\text{oc}})$$

where P_{max} is the maximum output electrical power.

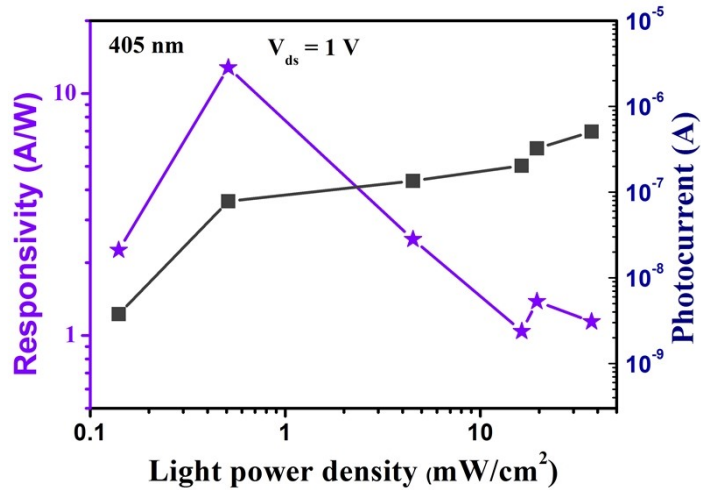


Figure S13. Responsivity and photocurrent as a function of light power density at the bias of 1 V.

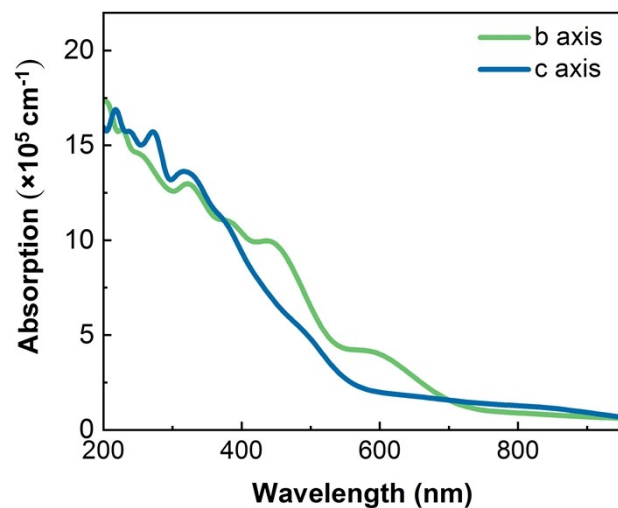


Figure S14. Calculated absorbance along b-axis and c-axis for $\text{SnS}_{0.5}\text{Se}_{0.5}$.

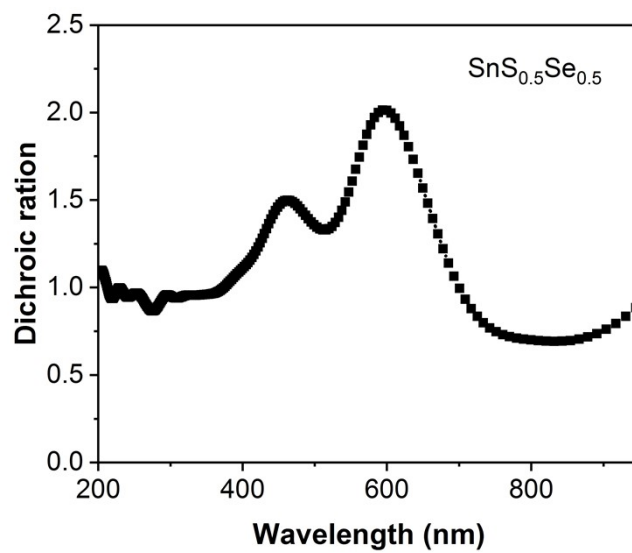


Figure S15. The dichroic ratio α_b/α_c extracted from $\text{SnS}_{0.5}\text{Se}_{0.5}$ absorbance.

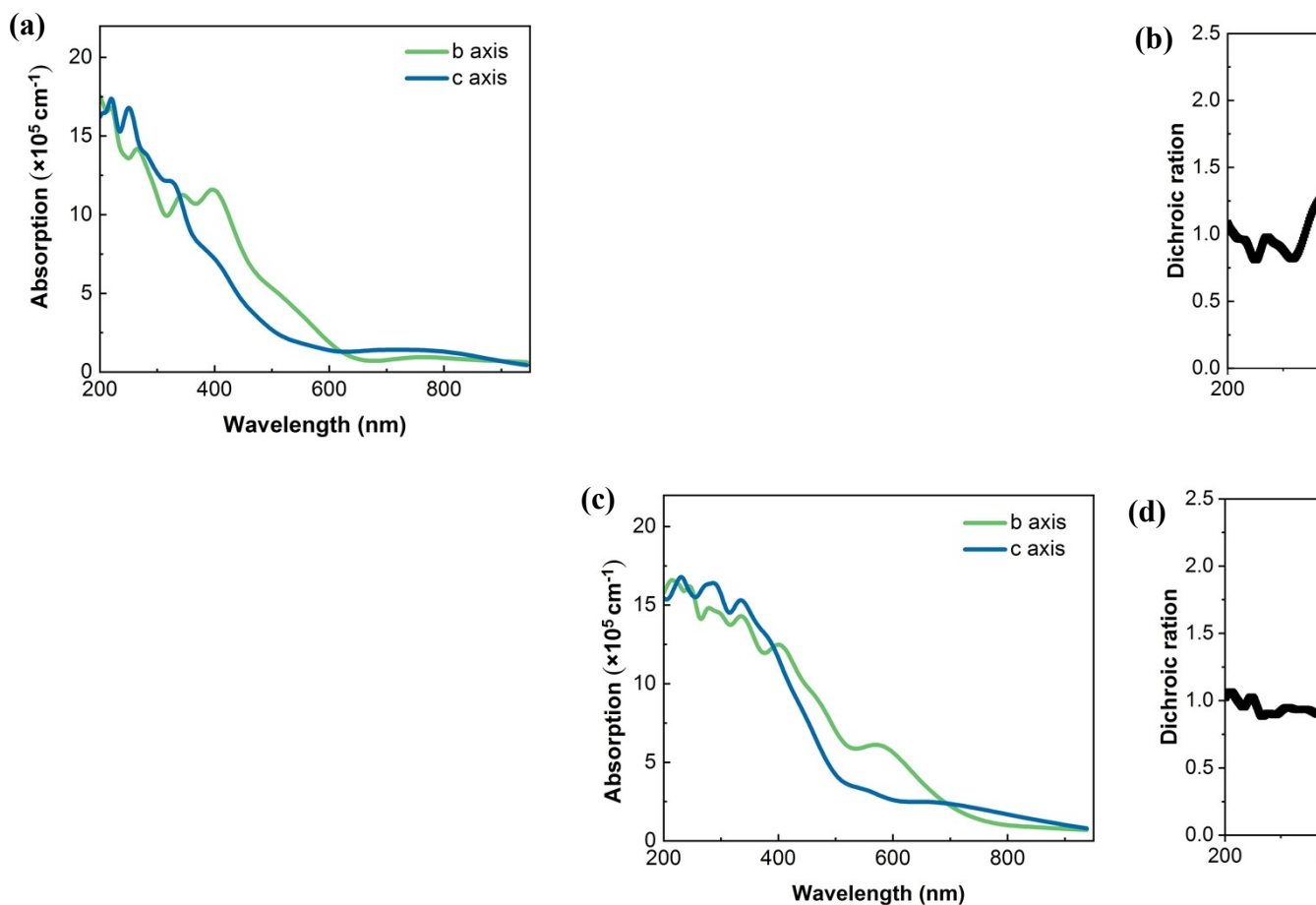


Figure S16. (a) Calculated absorbance along b-axis and c-axis for SnS. (b) The dichroic ratio α_b/α_c extracted from SnS absorbance. (c) Calculated absorbance along b-axis and c-axis for SnSe. (d) The dichroic ratio α_b/α_c extracted from SnSe absorbance.

References

1. J. D. Z. Yao, Z. Q.; Yang, G. W., *ACS Appl. Mater. Interfaces*, 2016, **8**, 12915-12924.
2. F. Wu, Q. Li, P. Wang, H. Xia, Z. Wang, Y. Wang, M. Luo, L. Chen, F. Chen, J. Miao, X. Chen, W. Lu, C. Shan, A. Pan, X. Wu, W. Ren, D. Jariwala and W. Hu, *Nat. Commun.*, 2019, **10**, 4663.